



Insights of the role of shell closing model and NICS in the stability of NbGe_n ($n = 7–18$) clusters: a first-principles investigation

Ravi Kumar Triedi^{1,2} and Debashis Bandyopadhyay^{3,*}

¹Department of Theoretical Physics, Institute Ruder Boskovic, 10000 Zagreb, Croatia

²Present address: Department of Physics, Presidency University, Bengaluru, Karnataka 560064, India

³Department of Physics, Birla Institute of Technology and Science, Pilani, Pilani, Rajasthan 333031, India

Received: 9 May 2018

Accepted: 22 August 2018

Published online:
31 August 2018

© Springer Science+Business
Media, LLC, part of Springer
Nature 2018

ABSTRACT

In the present report, the structures, energetics and electronic properties of neutral and cationic Nb-doped Ge_n ($n = 7–18$) clusters are systematically investigated under the first-principles density functional theory approach. The isomers in which the Nb atom is encapsulated inside a germanium cage are relatively stable compared to the exohedral surface doping. The thermodynamic stability and chemical activity of the ground-state isomers are analyzed through various energetic parameters. The results highlight the enhanced stability of the neutral NbGe₁₂ hexagonal prism-like structure with D_{6h} symmetry and cationic NbGe₁₆ fullerene isomers. The negative nucleus-independent chemical shift can explain the enhanced stability of neutral NbGe₁₂. However, the enhanced stability of cationic NbGe₁₆ is explained by shell closing model associated with the quasi-spherical geometry with a sequence $1S^21P^61D^{10}1F^61G^{12}2S^22P^61F^81G^62D^{10}$ following Hund's rule. To understand the effect of hybridization on stability, we have calculated density of states (DOS) and projected DOS (PDOS). From PDOS, it is clear that Nb-*p* and Ge-*s* and *p* orbitals are mainly take part in hybridization; however, near below Fermi level, the dominating contribution comes from Nb-*d* orbitals. In addition, IR and Raman spectra of clusters are also calculated to explain their vibrational properties of the isomers. Specifically, IR spectrum of the clusters in the range of 12–16 shows the possible application of these clusters in the IR sensing device.

Address correspondence to E-mail: debashis.bandy@gmail.com

Introduction

The electronic structure and stabilities of transition metal-doped semiconductor clusters are now interesting field of research for their potential application in the electronic industries. In the field of semiconductor materials research, transition metal-doped germanium clusters are an important alternative to the silicon clusters because of its larger electron number and hole mobility [1, 2]. However, pure germanium clusters are chemically reactive [3] and therefore are not suitable as a building block of assembled materials [4, 5]. The transition metal atoms absorb the unsaturated bonds present in the semiconductor clusters and form sp^3 hybridization to stabilize the cage clusters [6–9]. Sometimes, these hybrid clusters appear as thermodynamically stable magnetic clusters depending upon their composition [10, 11]. A large number of investigations on a transition metal-encapsulated semiconductor clusters with potential applications in semiconductor industries have been reported. At the early stages of the investigation on transition metal-doped semiconductor clusters, the main focus was to search for the globally stable clusters in a particular size and within a definite size range. In the later stage, the study shifted toward the search for the cause of the stability of the clusters in a particular size and composition following existing electron counting rule, shell closing model and measurement of nucleus-independent chemical shift (NICS) [7, 12–21]. There have been a number of other interesting findings reported on the metal-encapsulated germanium cage clusters. Jin et al. [6] performed a global minimum search for the multi-charged ruthenium-doped germanium clusters using density functional theory (DFT). A number of reports on electronic structures, stabilities and magnetic quenching of transition metal (TM)-doped silicon and germanium clusters (TM = Mo, Cr, Ni, Ti, Zr, Hf, Cu, etc.) are reported by Dhaka et al. [22] and Trivedi et al. [23] using DFT-based study with indication of possible formation of stable clusters and cluster-assembled materials. Kumar et al. [7] also studied the IR and Raman spectra to compare the vibrational nature of TM@Ge_n clusters (TM = Ti, Zr, Hf, $n = 1–20$). Recently, Trivedi and Bandyopadhyay [24] studied the vibration properties of Ag, Au-doped Ge and Si nanoclusters with specific geometry and shown that Ag and Au in

silicon cages are more preferable to the germanium clusters. Dhaka and Bandyopadhyay [25] studied the electronic structure, stability and magnetic quenching of CrGe_n ($n = 1–17$) using density functional theory. They explained the stability of CrGe₁₀ and CrGe₁₄ clusters due to the closed-shell filled structure. The mixing of Cr-*d* orbital with the *s* and *p* orbital of germanium is mainly responsible for the stability and quenching of the Cr magnetic moment. Similarly, WGe_n ($n = 1–17$) [26], AuGe_n ($n = 2–13$) [27] and MGe_n ($n = 9–10$, M = Si, Li, Mg, Al, Fe, Mn, Pb, Au, Ag, Yb, Pm and Dy) [28] also have been investigated by using density functional theory. Simultaneously, one can tune the wide range of electronic and structural properties by varying the doping element in semiconductor cage clusters. Bandyopadhyay et al. [29–32] investigated the electronic structure, growth behavior and different physical and chemical properties of TM metal-doped germanium cage clusters. Depending upon the doped transition metal atom, even a single-doped atom may significantly affect the stability of a semiconductor clusters and show magic behavior which is found by the anion photoelectron spectroscopy [33]. Electronic structure of both the anionic and neutral triatomic species was theoretically studied by Pham and Nguyen [34]. Recently, Kumar [9] studied the divalent metal (M)-atom-doped X_nM (X = Si, Ge and Sn, $n = 8–12, 14$) clusters and showed that the nine- and ten-atom-capped prism structures as well as 12 and 14 atom clusters can transform into magic clusters with higher symmetry and large HOMO–LUMO gap. Xia et al. [8] reported neutral and charged niobium-doped silicon clusters and found that anion NbSi₁₂ cluster is very stable in a high-symmetry endohedral D_{6h} structure in which Nb atom is placed at the center of a regular hexagonal prism of Si atoms. Li et al. [35] determined the structures of cationic NbSi_n ($n = 4–12$) using the combination of infrared phonon dissociation and density functional calculations. They found that the interaction with a Nb atom, with its partially unfilled 4*d* orbitals, leads to a significant stability enhancement of the Si_n framework as reflected. Kumar [36] studied the stability of germanium nanotubes doped with Nb, Mo and W, respectively, using density functional calculations and suggested the Nb-doped germanium nanotube having metallic characteristic. So searching for an Nb-doped germanium stable cluster is very interesting because it can be used as building blocks in the cluster-assembled

materials for various electronic and optical applications. In the present work, we have performed a global minimum search for the Nb-doped Ge_n ($n = 7\text{--}18$) neutral and cationic clusters using density functional theory. The size-dependent growth behavior, electronic properties and IR or Raman spectrum of the clusters are discussed. We have also calculated the nucleus-independent chemical shift (NICS) parameter to explain the enhanced stability of neutral NbGe_{12} hexagonal prism-like structure. Detailed analyses are performed for the density of states (DOS) based on shell closing model for explaining the stability of cationic NbGe_{16} clusters. Though there are many such reports on the explanation of the stability of the semiconductor clusters, still it needs more light to understand the systems for its potential applications in electronic industries as optical sensors and cluster-assembled materials. Therefore, the same question needs to address in the present system too.

Computational method

Geometrical structural optimization and frequency analysis of NbGe_n ($7\text{--}18$) clusters have been performed by using the DFT-B3LYP [37] functional and the LanL2DZdp for Ge and LanL2DZ (with effective core potential) for Nb atoms. While calculating DOS and PDOS using Vienna Ab Initio Simulation Package (VASP) computational code [38, 39] in order to avoid interaction between neighboring clusters, a large cubic cell of 40 Å edge lengths with a periodic boundary condition is taken. The k-grid integration has been carried using the Γ -point approximation. The atomic positions have been optimized by the conjugate gradients dynamics algorithm until the residual forces are smaller than 10^{-3} eV/Å, and without any symmetry constraints. Further analysis of the electronic properties and molecular orbitals has been performed with the software Gaussian '09 [40] using B3LYP and the Gaussian-type basis sets as mentioned. To search for the lowest energy structures of Nb-doped germanium clusters, a large number of possible initial geometries include one-, two- and three-dimensional configurations obtained by using the reported structures and Universal Structure Predictor: Evolutionary Xtalloraphy (USPEX) [41] to predict initial guess structures. All clusters are relaxed fully without any symmetry constraints. All

the structures have positive frequencies which indicate that all clusters are physically acceptable and therefore correspond to the potential energy minima. In addition, to explain the stability of NbGe_{12} hexagonal prism-like structure based on aromaticity, the nucleus-independent chemical shift (NICS) [42] was calculated by gauge-independent atomic orbital (GIAO) method. Calculated DOS and PDOS are also used to explain the shell closing model of cationic NbGe_{16} cluster which follow the sequence $1S^21P^61D^{10}1F^61G^{12}2S^22P^61F^81G^62D^{10}$ that follow the Hund's rule.

To justify the reliability of our calculations, the bond length (Å), vibrational frequency (ω) and vertical ionization potential of NbGe , Nb_2 and Ge_2 dimers are calculated using different density functional methods and the results as well as theoretical and experimental data summarized in Table 1. The Ge–Ge dimer has a ground state with bond length of 2.45 Å, frequency 267.50 cm^{-1} and first IP 6.44 eV, which is in excellent agreement with reported theoretical and experimental calculation [43, 44]. The Ge–Nb dimer with bond length 2.34 Å has agreement with the experimental result [45]. For Nb_2 dimer, the theoretical and experimental bond length and vibrational frequencies are 2.08 Å, 472 cm^{-1} [46] and 2.08 Å, 424.9 cm^{-1} [47], respectively, and are in good agreement with our theoretical observation. So the calculated results using B3LYP functional are closer to experimental and calculated theoretical data than other functional. Therefore, our calculated results are reasonably good to describe properties of NbGe_n clusters.

Results and discussion

To check the reliability of our computation, first we have calculated different parameters, bond length, ionization potential, etc., of the Ge–Ge, Ge–Nb and Nb–Nb diameters calculated. The calculated results perfectly matched with theoretical and experimental results. We summarized the calculated results and compared with experimental data, which is shown in Table 1. We can wrap up that our calculated results based on B3LYP method and the basis sets as mentioned in computation section are very close to the experimental results. So our computational scheme is logically good to describe these clusters.

Table 1 Bond length, frequency and first IP of Ge–Ge, Ge–Nb and Nb–Nb dimer

Dimer	Methods	Bond length (Å)	Frequency (cm ⁻¹)	First IP (eV)	Experimental values		
					Bond length (Å)	Frequency (cm ⁻¹)	IP (eV)
Ge–Ge	B3LYP	2.456	267.5	6.45	2.46 [43]	258 [44]	7.89 ^a
	MPW1PW91	2.456	267.5	6.65			
	B3PW91	2.455	267.6	6.69			
Ge–Nb	B3LYP	2.345	305.9	5.90	2.35 [45]		
	MPW1PW91	2.346	306.2	6.14			
	B3PW91	2.335	306.5	5.44			
Nb–Nb	B3LYP	2.093	472.33	5.94	2.08 [46, 47]	424–472 [46, 47]	6.74 ^a
	MPW1PW91	2.074	485.92	6.02			
	B3PW91	2.10	480.15	5.99			

^aNIST atomic spectra database

Geometrical structures of pure Ge_n clusters

Based on the previous reports, we have recalculated the pure germanium clusters using B3LYP functional. It is worth to mention here that Tai and Nguyen [48] adopted a stochastic search method that covers a good number of isomeric structures of pure germanium clusters and increases the chance of finding the ground-state geometry. In the present work, we have also found similar kinds of structures which are comparable to their report. The ground-state isomer of the Ge₃ cluster is a C_{2v} triangular geometry, while the addition of another Ge atom changes the structure to a bend rhombus structure with D_{2h} symmetry. The Ge₅ cluster is a triangular bipyramid with D_{3h} symmetry. The Ge₆ is a bi-capped rectangular geometry with D_{4h} symmetry. The most stable isomer of the Ge₇ is bi-capped pentagonal structure having C₂ point group symmetry. The ground-state structure of Ge₈ cluster is nearly a capped pentagonal bipyramid with C_s symmetry. The Ge₉ cluster forms a capped cube-like structure with C_{4v} symmetry. For Ge₁₀, the most stable structure is a two-sided capped Ge₈ cubic structure with C₁ symmetry. Ge₁₁ is a capped pentagonal prism structure with C_{2v} point group symmetry. Ge₁₂ ground-state isomer is a bend hexagonal prism with D_{3h} symmetry. With the increasing size, the structures of pure Ge clusters divert from the symmetrical shape and can be assigned with C₁ symmetry. The ground-state Ge₁₃ is a capped hexagonal prism-like Ge₁₂ structure. Ge₁₄ is relatively symmetric. It is a combination of three rhombi and six pentagons. Four pentagons are connected with each rhombus. The Ge₁₅ is a rectangular

tube structure capped with a Ge atom. Ge₁₆ ground state is different from cage structure. It is a combination of two Ge₈ clusters in the form of cluster assembly. Ge₁₇ also is a combination of Ge₁₀ and Ge₇. Ge₁₈ is similar to the structure of ground-state Ge₁₄ isomer. It is a combination of two rhombi, eight pentagons and one hexagon. The next large-sized structure Ge₁₉ looks like a mask with one Ge atom is endohedral doped. Ge₂₀ ground structure is again a combination of two identical Ge₁₀ bi-capped rectangular prism-like structures.

Geometrical structures of NbGe_n clusters

The goal of this section in the present study is looking at the relevant features related to the geometric, electronic and vibrational properties of the NbGe_n (*n* = 7–18) clusters. Using the computational scheme, as described in the “Computational method” section, we have explored many low-lying isomers with *n* > 6 and selected the ground-state isomer in each size. Stable isomers along with other low-lying isomers with point group symmetry of clusters are shown in Fig. 1. [All other additional ground-state structures of neutral and charged clusters are shown in supplementary information A and A1, respectively]. The ground-state structure of NbGe₇ is a distorted cube with C_s symmetry. Here, the Nb atom absorbs over the surface of the Ge₇ pure cluster. Other two next low-lying isomers are at 0.29 eV and 0.44 eV higher in neutral state compared to the ground-state structure. The ground-state NbGe₈ structure is Nb-capped cubic Ge₈ structure. So, Nb atom is completely exposed. In NbGe₉, the Nb atom absorbs partially

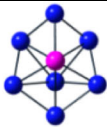
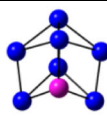
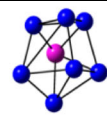
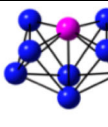
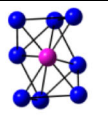
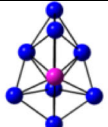
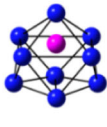
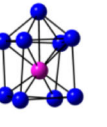
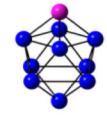
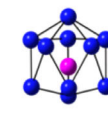
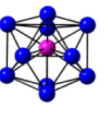
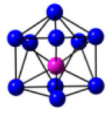
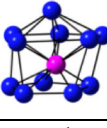
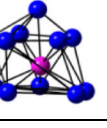
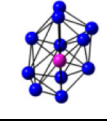
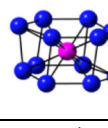
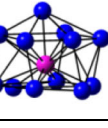
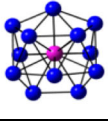
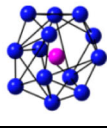
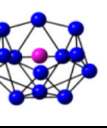
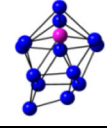
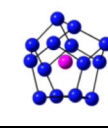
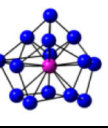
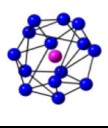
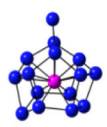
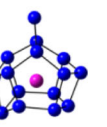
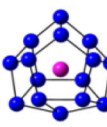
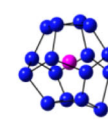
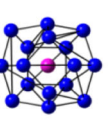
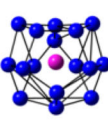
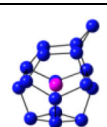
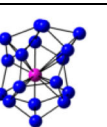
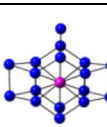
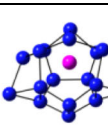
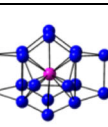
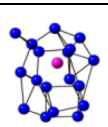
Cluster	Ground state	Low energy isomers		Cluster	Ground state	Low energy isomers	
Ge ₇ Nb				Ge ₈ Nb			
	C _s ¹	ΔE=0.29	ΔE=0.44		C _s ¹	ΔE=0.24	ΔE=0.45
Ge ₉ Nb				Ge ₁₀ Nb			
	C ₁ ¹	ΔE = 0.37	ΔE=0.85		C ₂ ¹	ΔE = 0.07	ΔE = 0.09
Ge ₁₁ Nb				Ge ₁₂ Nb			
	C _s ¹	ΔE = 0.02	ΔE = 1.33		C ₁ ¹	ΔE = 0.67	ΔE = 0.93
Ge ₁₃ Nb				Ge ₁₄ Nb			
	C _s ¹	ΔE = 0.27	ΔE = 0.84		C _s ¹	ΔE = 0.02	ΔE = 0.07
Ge ₁₅ Nb				Ge ₁₆ Nb			
	C ₂ ¹	ΔE = 0.04	ΔE = 0.19		C ₂ ¹	ΔE = 0.30	ΔE = 0.57
Ge ₁₇ Nb				Ge ₁₈ Nb			
	C ₁ ¹	ΔE = 1.31	ΔE = 2.67		C ₁ ¹	ΔE = 0.37	ΔE = 1.58

Figure 1 Optimized ground-state structures of NbGe_n (*n* = 7–18) clusters with point group symmetry. Blue balls are Ge and pink balls are Nb atoms. Superscripts in point group symmetry present the spin state of ground-state structures.

inside the Ge₉ cages. The next two low-lying clusters are 0.24 eV and 0.45 eV higher in energy compared to the ground state. The optimized ground state of NbGe₉ is a modification over ground-state NbGe₈ structure. In the cage of NbGe₈, Nb is replaced by additional Ge and Nb atom which absorbs partially inside the Ge₉ cage. Again by replacing Nb by Ge in NbGe₉, it gives Ge₁₀ cage where Nb absorbs completely endohedral. The addition of one Ge atom, NbGe₁₀ ground-state cluster, converted to a structure where Nb atom sandwiched between two pentagonal surfaces and one surface is capped by a Ge atom with C_s symmetry. The immediate higher NbGe₁₂ ground state is a hexagonal prism-like structure where the

endohedral doped Nb atom hybridized with all Ge atoms in the cage. The other low-energy isomers are distorted icosahedral and fullerene kinds. The geometry of ground-state isomer NbGe₁₃ can be understood after capping three germanium atoms at different surfaces of NbGe₁₀ ground-state isomer. Ground-state NbGe₁₄ is well-known structure and is a combination of six pentagons and three rhombi. The geometry of NbGe₁₅ is a modification of the ground-state NbGe₁₀ structure where five additional germanium atoms are added in the form of two Ge–Ge dimers and one germanium atom at different places. NbGe₁₆ ground state is again fullerene kind of structure and is a combination of ten pentagons and

two rhombi. The structure can be understood by adding a Ge–Ge dimer at the top of NbGe₁₄ ground state. By adding one Ge atom with the one of the rhombus in NbGe₁₆ and then after optimization, one can get NbGe₁₇ ground-state structure. NbGe₁₈ is a flying disk-like structure where the central part is pentagonal prism kind. Most of these geometries have already been reported for other systems obtained by global optimization methods.

Stabilities of NbGe_n clusters

To identify a stable cluster in a particular composition, it is necessary to study the variations of different thermodynamic and chemical parameters from the ground-state energy of different clusters in different charge states. These parameters are binding energy (BE), fragmentation energy (FE), stability or second-order energy difference (Δ_2), HOMO–LUMO gap, ionization potential (IP), electron affinity (EA), etc., and can be compared between different cluster sizes during the growth process. In the present investigation, we have studied NbGe_n ($n = 7–18$) clusters in neutral and cationic states.

To explore the relative stability of the clusters with the increase in the cluster size during the growth process, we have calculated different thermodynamic and chemical parameters. The average binding energy per atom (BE), stability and fragmentation energy (FE) are calculated following our previous reports [22–25]. These parameters are defined as:

$$BE = (E_{\text{Nb}} + nE_{\text{Ge}} - E_{\text{NbGe}_n}) / (n + 1)$$

$$FE = E_{\text{NbGe}_{n-1}} + E_{\text{Ge}} - nE_{\text{NbGe}_n}$$

$$\begin{aligned} \Delta_2 &= (E_{\text{NbGe}_{n+1}} - E_{\text{NbGe}_n}) - (E_{\text{NbGe}_n} - E_{\text{NbGe}_{n-1}}) \\ &= E_{\text{NbGe}_{n+1}} + E_{\text{NbGe}_{n-1}} - 2E_{\text{NbGe}_n} \end{aligned}$$

where E_{Nb} , E_{Ge} , E_{Ge_n} and E_{NbGe_n} represent the energies of Nb, Ge, Ge_n and NbGe_n, respectively. The variation of average binding energy is shown in Fig. 2a. The BE as well as the increase rate of BE for $n = 7–12$ is relatively higher in both neutral and cationic NbGe_n clusters compared to the pure Ge_n series. This indicates that the doping of Nb atom increases the BE and helps to improve the stability of the clusters. Visible local peaks at $n = 12$ for neutral and $n = 16$ in cationic clusters indicate the enhanced stability of these clusters in the respective series (in addition, the variation of binding energy of neutral, cation and anion is shown in supplementary information SI-B).

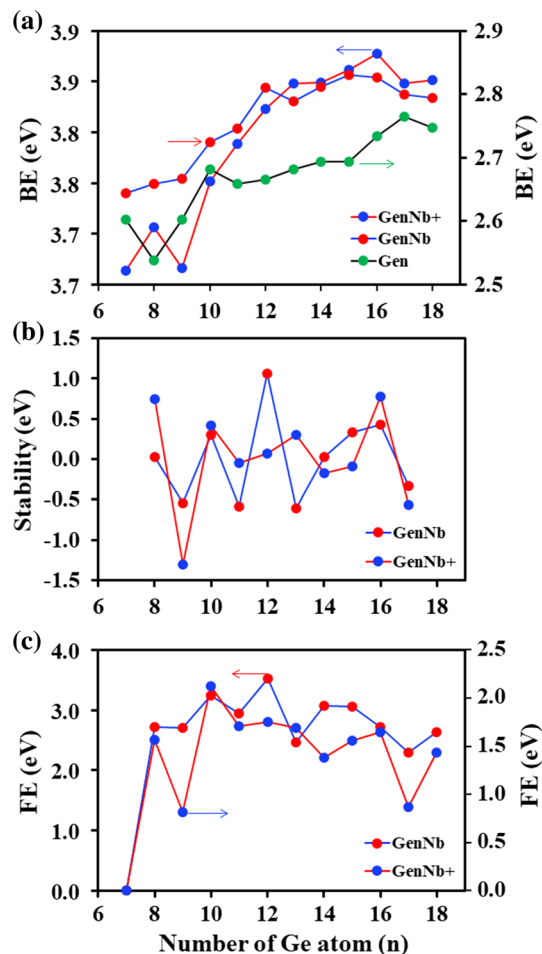


Figure 2 Variation of **a** averaged binding energies (BE), **b** second-order change in energy (Δ_2) and **c** fragmentation energy (FE) of NbGe_n⁺ and NbGe_n ($n = 7–18$) clusters with the number of germanium atom.

To further check stability of the clusters, we calculate the stability and fragmentation energies of different clusters. Expression of stability is basically representing the second-order change in energy, whereas the expression of the fragmentation energy indicates the stability of the cluster. As seen from Fig. 2b, neutral clusters with $n = 10$ and 12 and cationic clusters with $n = 13$ and 16 show local maxima. The relatively high change in second-order change in energy could be related to the formation of stable cage structure. The cluster with higher value of fragmentation energy needs more energy to dissociate it. The variation of stability and fragmentation energies with the size of clusters (number of germanium atoms, n) is shown in Fig. 2. The FE rises from $n = 11–12$ and drops from $n = 12–13$ during the growth process. These indicate that NbGe₁₂ cluster is

relatively stable compared to its neighboring sizes. The same is true for cationic NbGe_{16} cluster. There are wide ranges of variations in the HOMO–LUMO gap with a number of ups and downs. From this nature, it is difficult to identify the chemically stable clusters. However, comparing this nature with the ionization energy (or ionization potential) variation, one can select neutral NbGe_{12} and cationic NbGe_{16} clusters as the chemically stable clusters. This selection with the variation of thermodynamic parameter variation, select neutral NbGe_{12} and cationic NbGe_{16} clusters are globally stable clusters. We define ionization energy (or ionization potential) as follows:

$$\text{VIE (or AIE)} = E_{\text{NbGe}_n^+} - E_{\text{NbGe}_n}$$

By definition, vertical ionization energy (VIE) is the energy difference between the cationic and neutral clusters, where the cationic cluster is at the same equilibrium geometry of the neutral cluster, whereas adiabatic ionization energy (AIE) is defining the energy difference between the neutral and its cationic clusters and both are at the same equilibrium geometry of the cationic cluster. Ionization of a molecule or a cluster often changes its geometry on ionization. It is to be noted that the variation in VIE and AIE is almost similar to the variation of size of the cluster. This is an indication that hardly there is any structural variation due to ionization of the neutral clusters. Therefore, we have calculated both AIE and VIE values in the present study. Calculated results are shown in Fig. 3b, c (see also Table 2 in SI). Both IPs are almost same at all sizes (with a sharp peak at $n = 12$) indicating that the cluster geometries remain same after ionization. The analysis indicates that both VIE and AIE increase sharply for $n = 11$ – 12 . Both VIP and AIP trends support the enhanced stability of neutral NbGe_{12} cluster in the series. We have also calculated the charge transfer and bond length parameter which may play an important role in defining the stability and geometry of the clusters. Both parameter as a function of cluster size is shown in supplementary information SI-C and SI-D, respectively. In summary, from the variation of the thermodynamic parameters and chemical parameters, one may found that NbGe_{12} and NbGe_{16}^+ clusters have enhanced stability.

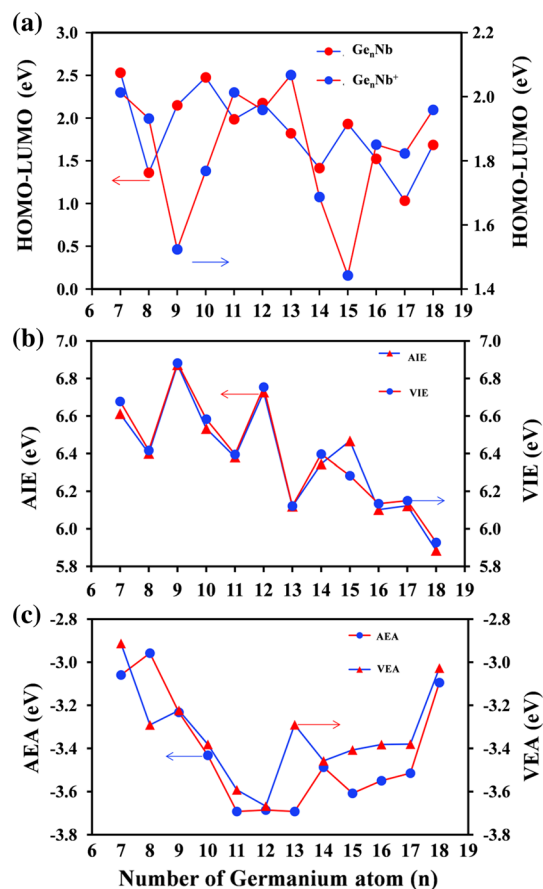


Figure 3 Variation of **a** HOMO–LUMO gap, **b** vertical ionization energy (VIE), adiabatic ionization energy (AIE) and **c** vertical electron affinity (VEA), adiabatic electron affinity (AEA) of the NbGe_n clusters with number of germanium atom.

Nucleus-independent chemical shift (NICS) of NbGe_{12} cluster

Further, to understand the cause of the stability of NbGe_{12} , we have calculated nucleus-independent chemical shift (NICS) parameter. In chemistry and in cluster science, the aromaticity is a key concept [49] to understand the stability. The aromatic behavior of a cluster is the measure nucleus-independent chemical shift (NICS) index and is defined as the negative value of the magnetic shielding, computed at the ring center (as like benzene ring) or at some other selected point. Chen et al. [42] reported the NICS approach as aromaticity criteria based on magnetic properties, which have been applied to characterize the metallic clusters with aromatic and antiaromatic nature. The rings with more negative values are considered as more aromatic species and hence with enhanced stability nature. However, positive and zero NICS

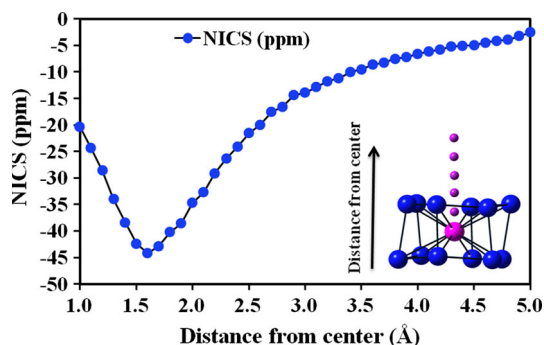
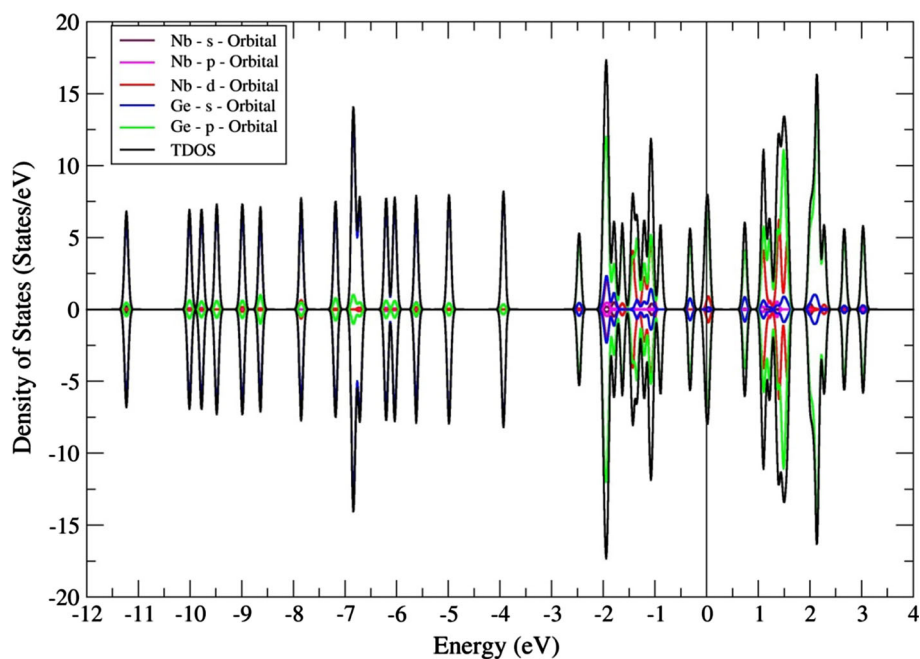


Figure 4 Nucleus-independent chemical shift (NICS) variations of NbGe_{12} cluster with the distance from center.

values indicate antiaromatic and non-aromatic species. Using the GIAO-B3LYP/Lan12dz method with effective core potential, we have calculated NICS values. The variation of NICS values of NbGe_{12} cluster are shown in Fig. 4. Calculated NICS values close to the outer surface are relatively smaller than the NICS values inside the cage. Calculated NICS variation with the distance from the central Nb atom shows a minimum value of -44.89 ppm at a distance 1.5 Å above from the center of the cluster. Aromaticity in hexagonal structure like benzene is an important conformation of stability of NbGe_{12} cluster. With reference to our previous work [23] on MoGe_{12} , the size variation of NICS supports the aromatic nature and hence enhanced stability of neutral NbGe_{12} cluster. However, in the cationic series, there

Figure 5 Electron density of states of NbGe_{16}^+ cluster **a** total DOS, **b** contribution of Ge s, p and Nb-s, p, and d orbital in total DOS.



is no such evidence that could explain the stability of the cationic clusters. We did not calculate NICS values of the other clusters because they are not stable as we discuss in relative stability section. We have calculated NICS value of NbGe_{12} only just because of predicting aromatic character of this cluster which is one of the main causes of its enhanced stability.

Shell model of cationic NbGe_{16}

A number of reports are there to explain the enhanced stability of the clusters using the closed-shell model [50–53]. It has already been reported that in FeMg_8 cluster, partially filled sub-shells can enhance chemical stability [51] with a closed core of $1S^2, 1P^6, 1D^{10}, 2S^2$ superatomic shells followed by a crystal-field split $2D^4$ valence state resulting in a magnetic moment of $4.0 \mu_B$. Khanna and Jena [52] proposed that the stable clusters could be treated as superatoms that form a third dimension to the periodic table. Kumar [53] studied doping of different divalent Mn atoms and report the finding of Mn-doped Ge and Sn clusters with $5 \mu_B$ magnetic moment in accordance with the Hund's rule in clusters. In VLi_8 magnetic superatom, Zhang et al. [54] found a filled d sub-shell with a magnetic moment of $5 \mu_B$ with $1S^2 1P^6 1D^5$ electronic distributions. In the present report to understand the magic nature of cationic NbGe_{16} cluster, we have calculated the density of states (DOS) and partial orbital contributions

in total DOS (PDOS) of the NbGe₁₆ clusters in cationic states in Fig. 5.

From the atomic orbital contribution in total DOS, it is clearly seen that most of the contribution in the total density of states is from Nb *d* orbital (red color) and from *p* orbitals (green color) of all Ge atoms. Therefore, Nb *d* orbital is mainly taking part in hybridization to make the cluster stable. Again, the HOMO–LUMO gap of NbGe₁₆ is more in the cationic states (1.8 eV) compared to the neutral clusters (1.5 eV). We have presented the complete sequence of the single-electron orbitals in Fig. 5. Due to finite broadening during the calculation of DOS, closely spaced orbitals are taken as one in DOS, and on the basis of it, we have assign the orbitals as shown. We found that cationic NbGe₁₆ cluster follows the orbital sequence $1S^21P^61D^{10}1F^61G^{12}2S^22P^61F^81G^62D^{10}$ in

Fig. 6 and adjusts totally 68 electrons as like closed-shell filled number.

We have also calculated the one-electron energy level and orbital iso-surface to show interaction between transition metal and Ge cage as shown in Fig. 6. The electronic structure of NbGe₁₆ cation accounts for a total of 68 delocalized valance electrons (4 electrons form each Ge and 4 electrons form the Nb atom) arranged in $1S^21P^61D^{10}1F^61G^{12}2S^22P^61F^81G^62D^{10}$ in accordance with closed-shell configurations as shown by the one-electron energy levels and molecular orbitals iso-surfaces in Fig. 6. There is a significant interaction between the transition metal atom and the Ge cage. Further due to crystal-field splitting, some of the lower orbitals appear at the higher energy levels as shown in the sequence. This is one of the strongest evidence of the insight of the

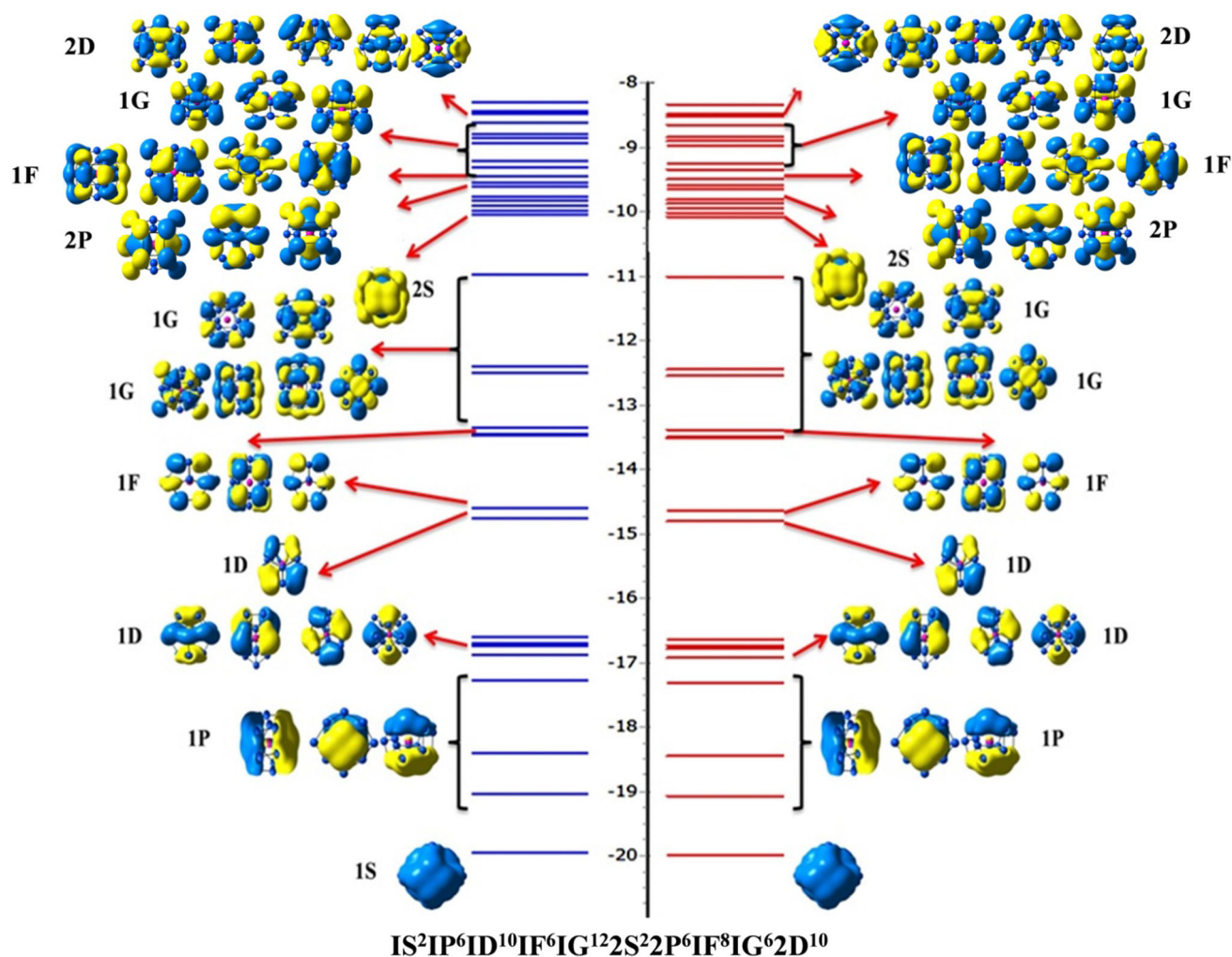


Figure 6 One-electron energy level and molecular orbital iso-surface of cationic NbGe₁₆ (blue color showing positive diffuse and yellow color showing negative diffuse).

stability of cationic NbGe_{16} cluster as reported by others [32], and hence, NbGe_{16}^+ can be taken as a superatom with very high embedding energy 10.58 eV, IP (10.25 eV) and HOMO–LUMO gap of 1.85 eV.

IR and Raman spectra

To understand the vibrational properties of the ground-state clusters, IR and Raman spectra of the optimized geometries are calculated and shown in Fig. 7. The absence of any imaginary frequency in the spectrum represents the real nature of the clusters. It also indicates that there is no transition state in any of the ground-state isomers. The dominant peaks shown in the IR and Raman spectra are due to the vibration of the atoms in the cage. Careful observation shows the presence of mainly three to four dominating modes in IR and Raman spectra for all clusters. A lower number of vibrational modes in IR are basically the indication of the vibration of the bonds (stretching) present in the structure nearly at the same frequency or within a very narrow frequency range. This is because of the strong structural symmetry of these clusters. Raman frequency in general indicates the bending mode in the clusters. The dominating higher mode frequency with very high intensity is the breathing mode of the cage cluster atoms similar to the work done by Bandhyopadhyay [7], while the IR intensities have three or four peaks in neutral and cationic cluster corresponding to the motion of Nb atom in different directions. In the breathing mode, all Ge atoms vibrate in the same phase, whereas the doped atom remains static. The frequency region, which is less than 200 cm^{-1} , is mainly due to the vibration of the germanium atoms and the doped atom as well. This frequency mode shifted toward the low-frequency region except for $n = 12$ structure. Also for $n = 14$ and 15 the dominant peaks in the infrared spectrum shifted toward lower frequencies suggesting that the Ge–Nb bonds become relatively weak as the size of the cluster grows. The data of infrared spectrum of NbGe_n ($n = 10$ –15) are shown in supplementary information (SI) in Table 2. Gaussian broadened of different ground-state clusters ($n = 10, 12, 14$ and 15) to check the stability is shown in supplementary information (SI-E). Closer observation of the dominating mode frequencies in both IR and

Raman spectra, it is found that the infrared spectrum of NbGe_{12} has dominant peak at around 251 cm^{-1} due to additional strength in bonding because of NICS behavior. The high-frequency region indicates the higher bond energy between the elements. Comparing this with the binding energy graph, it can be said that the increase in bond energies helps to increase the binding energy per atom in the clusters. So, IR and Raman activities show distinct spectra of these clusters and reflect the effect of structural change and bonding nature. Now comparing to the far-infrared range, which is approximately 400 – 10 cm^{-1} (25 – $1000\text{ }\mu\text{m}$), it appears in the IR range of the present isomers. Therefore, the ground-state clusters with the composition could be useful for IR sensing device in the far-infrared region.

Conclusions

In summary, we have theoretically studied the electronic structure, vibrational properties and superatomic behavior of Nb-doped germanium clusters at different sizes in neutral and cationic states. Different thermodynamic and chemical parameters of the clusters show that neutral NbGe_{12} and cationic NbGe_{16} are the most stable species in the whole range of study. We have further applied NICS on neutral NbGe_{12} and closed-shell model on cationic NbGe_{16} ground-state clusters. We found that the NICS behavior of the ground-state NbGe_{12} cluster supports the aromatic nature of this cluster with a minimum NICS value of -44.89 ppm , while cationic NbGe_{16} follows the closed-shell superatomic model with the orbital sequence $1S^21P^61D^{10}1F^61G^{12}2S^22P^61F^81G^62D^{10}$ to accommodate 68 electrons which is a shell closing number. The large HOMO–LUMO gap of 1.85 eV makes this cluster chemically stable and suitable for application as optoelectronic devices. Further, the absence of any imaginary frequencies in these clusters shows that there is no presence of imaginary bonds in the clusters and clusters can be physically acceptable. These clusters could be useful for IR sensing device in the far-infrared region. Therefore, Nb-doped germanium stable cluster is very interesting because it can be used as building blocks in the cluster-assembled materials for various electronic and optical applications.

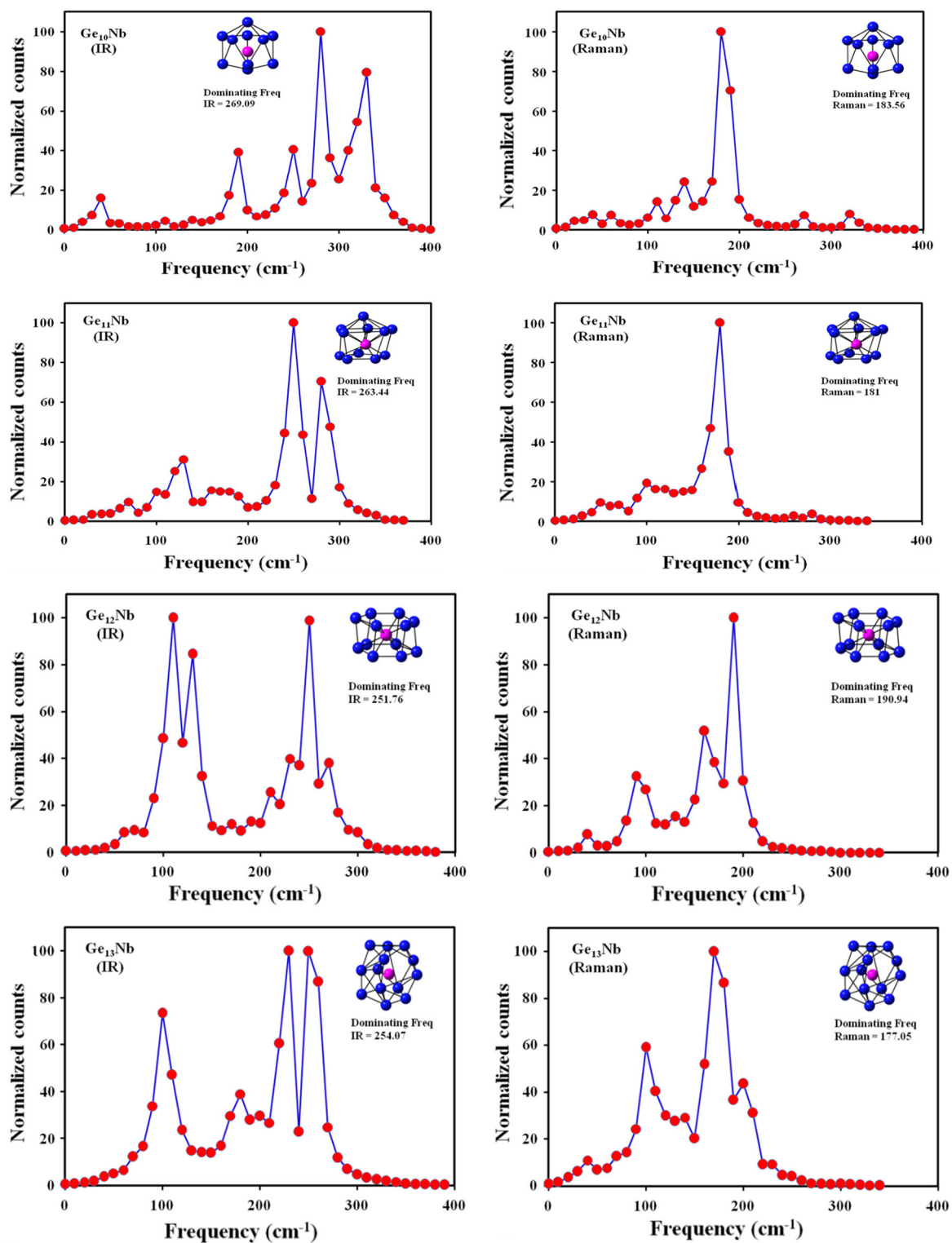


Figure 7 IR and Raman spectra of neutral NbGe_n (*n* = 10–16) clusters.

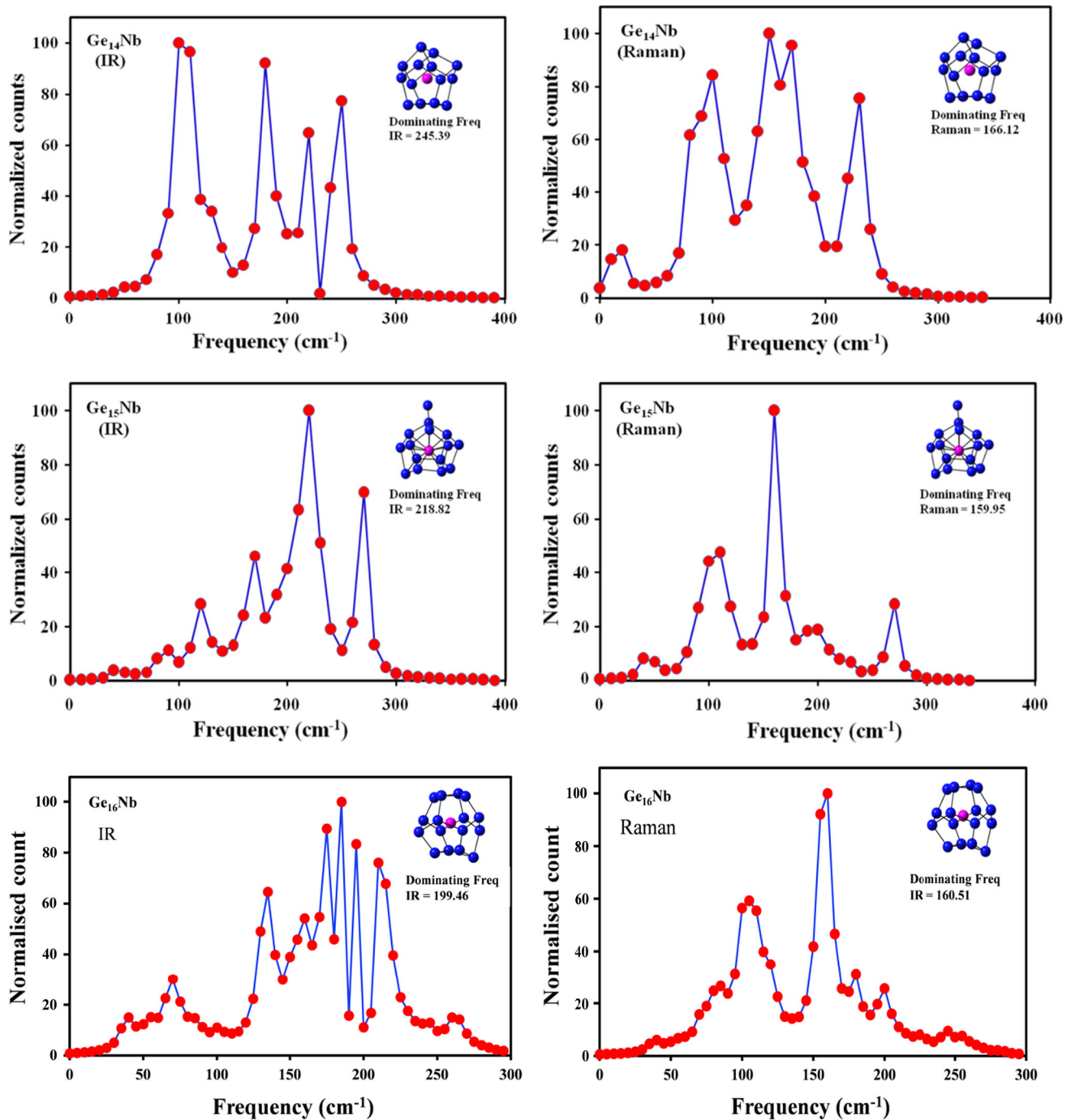


Figure 7 continued.

Acknowledgements

Complete Structural optimizations using Gaussian '09 were performed at the Birla Institute of Technology and Science Pilani, Rajasthan, India. The density of states calculation was performed by using Malnar clusters in IRB (Institute Ruder Boskovic) at Zagreb, Croatia.

Author contributions

RT and DB conceived the idea, performed the calculations and written the manuscript.

Electronic supplementary material: The online version of this article (<https://doi.org/10.1007/s108>

53-018-2858-3) contains supplementary material, which is available to authorized users.

References

- [1] Kamata Y (2008) High-K/Ge mosfets for future nanoelectronics. *Mater Today* 11:30–38
- [2] Pillarisetty R (2011) Academic and industry research progress in germanium nanodevices. *Nature* 479:324–328
- [3] Jarrold MF, Bower JE (1992) Mobilities of silicon cluster ions: the reactivity of silicon sausages and spheres. *J Chem Phys* 96:9180–9190
- [4] Wang L, Zhao J (2008) Competition between supercluster and stuffed cage structures in medium sized Ge_n ($n = 30–39$) clusters. *J Chem Phys* 128:024302. <https://doi.org/10.1063/1.2821106>
- [5] Wang J, Wang G, Zhao J (2001) Structure and electronic properties of Ge_n ($n = 2–25$) clusters from density functional theory. *Phys Rev B* 64:205411–205415
- [6] Jin Y, Tian Y, Kuang X, Lu C, Cabellos JL, Mondal S, Merino G (2016) Structural and electronic properties of ruthenium doped germanium clusters. *J Phys Chem C* 120:8399–8404
- [7] Kumar M, Bhattacharya N, Bandyopadhyay D (2012) Architecture, electronic structure and stability of $TM@Ge_n$ ($TM = Ti, Zr$ and Hf ; $n = 1–20$) clusters: a density functional modeling. *J Mol Model* 18:405–418
- [8] Xia XX, Herman A, Kuang XY, Jin YY, Lu C, Xing XD (2015) Study of the structural and electronic properties of neutral and charged niobium-doped silicon clusters: niobium encapsulated in silicon cages. *J Phys Chem C* 120:677–684
- [9] Kumar V, Kawazoe Y (2003) Metal-doped magic clusters of Si, Ge, and Sn: the finding of a magnetic superatom. *Appl Phys Lett* 83:2677–2679
- [10] Kapila N, Garg I, Jindal VK, Sharma H (2012) First principle investigation into structural, growth and magnetic properties in Ge_nCr clusters for $n = 1–13$. *J Magn Mater* 324:2885–2893
- [11] Zhurkin EE, Hou M (2000) Structural and thermodynamic properties of elemental and bimetallic nanoclusters: an atomic scale study. *J Phys Condens Matter* 12:6735–6754
- [12] Zhao WJ, Wang YX (2008) Geometries, stabilities, and electronic properties of $FeGe_n$ ($n = 9–16$) clusters: density-functional theory investigations. *Chem Phys* 352:291–296
- [13] Zhao WJ, Wang YX (2009) Geometries, stabilities, and magnetic properties of $MnGe_n$ ($n = 2–16$) clusters: density-functional theory investigations. *J Mol Struct Theochem* 901:18–23
- [14] Lu J, Nagase S (2003) Metal-doped germanium clusters MGe_n at the sizes of $n = 12$ and 10 : divergence of growth patterns from the $MSin$ clusters. *Chem Phys Lett* 372:394–398
- [15] Kapila N, Jindal VK, Sharma H (2011) Structural, electronic and magnetic properties of $MnCo, Ni$ in Gen for ($n = 1–13$). *Phys B* 406:4612–4619
- [16] Hou XJ, Gopakumar G, Lievens P, Nguyen MT (2007) Chromium-doped germanium clusters $CrGe_n$ ($n = 1–5$): geometry, electronic structure, and topology of chemical bonding. *J Phys Chem A* 111:13544–13553
- [17] Bandyopadhyay D, Sen P (2010) Density functional investigation of structure and stability of Gen and $GenNi$ ($n = 1–20$) clusters: validity of the electron counting rule. *J Phys Chem A* 114:1835–1842
- [18] Wang J, Han JG (2005) A computational investigation of copper-doped germanium and germanium clusters by the density-functional theory. *J Chem Phys* 123:244303. <https://doi.org/10.1063/1.2148949>
- [19] Wang J, Han JG (2006) A theoretical study on growth patterns of Ni-doped germanium clusters. *J Phys Chem B* 11:7820–7827
- [20] Wang J, Han JG (2008) Geometries, stabilities, and vibrational properties of bimetallic Mo_2 -doped Gen ($n = 9–15$) clusters: a density functional investigation. *J Phys Chem A* 112:3224–3230
- [21] Jing Q, Tian FY, Wang YX (2008) No quenching of magnetic moment for the $GenCo$ ($n = 1–13$) clusters: first principles calculations. *J Chem Phys* 128:124319. <https://doi.org/10.1063/1.2898880>
- [22] Dhaka K, Trivedi R, Bandyopadhyay D (2012) Electronic structure and stabilities of Ni-doped germanium nanoclusters: a density functional modeling. *J Mol Model* 19:1473–1488
- [23] Trivedi R, Dhaka K, Bandyopadhyay D (2014) Study of electronic properties, stabilities and magnetic quenching of molybdenum doped germanium clusters. *RSC Adv* 4:64825–64834
- [24] Trivedi R, Bandyopadhyay D (2018) Evolution of electronic and vibrational properties of $M@X_n$ ($M = Ag, Au, X = Ge, Si, n = 10, 12, 14$) clusters—a density functional modeling. *J Mater Sci* 53:8263–8273. <https://doi.org/10.1007/s10853-018-2002-4>
- [25] Dhaka K, Bandyopadhyay D (2015) Study of electronic structure, stability and magnetic quenching of $CrGe_n$ ($n = 1–17$) clusters: a density functional investigation. *RSC Adv* 5:83004–83012
- [26] Wang J, Han JG (2006) Geometries and electronic properties of the tungsten-doped germanium clusters: WGe_n ($n = 1–17$). *J Phys Chem A* 110:12670–12677
- [27] Li XJ, Su KH (2009) Structure, stability and electronic property of the gold-doped germanium clusters: $AuGe_n$ ($n = 2–13$). *Theor Chem Acc* 124:345–354

- [28] Qin W, Lu WC, Xia LH, Zhao LZ, Zang QJ, Wang CZ, Ho KM (2015) Structures and stability of metal doped Ge_nM ($n = 9, 10$) clusters. *AIP Adv* 5:067159. <https://doi.org/10.1063/1.4923316>
- [29] Bandyopadhyay D, Sen P (2010) Density functional investigation of structure and stability of Ge_n and Ge_nNi ($n = 1\text{--}20$) clusters: validity of electron counting rule. *J Phys Chem* 114:1835–1842
- [30] Bandyopadhyay D (2008) A DFT-based study of the electronic structures and properties of cage like metal doped silicon clusters. *J Appl Phys* 104:084308–084317
- [31] Bandyopadhyay D (2009) The study of electronic structures and properties of pure and transition metal doped silicon nanoclusters: a density functional theory approach. *Mol Simul* 35:381–394
- [32] Bandyopadhyay D (2009) Study of pure and doped hydrogenated germanium cages: a density functional investigation. *Nanotechnology* 20:275202. <https://doi.org/10.1088/0957-4848/20/27/275202>
- [33] Atobe J, Koyasu K, Furusea S, Nakajima A (2012) Anion photoelectron spectroscopy of germanium and tin clusters containing a transition-or lanthanide-metal atom; $\text{MGe}(n)$ - ($n = 8\text{--}20$) and $\text{MSn}(n)$ - ($n = 15\text{--}17$) ($M = \text{Sc-V, Y-Nb, and Lu-Ta}$). *Phys Chem Chem Phys* 14:9403–9410
- [34] Pham LN, Nguyen MT (2017) Titanium digermanium: theoretical assignment of electronic transitions underlying its anion photoelectron spectrum. *J Phys Chem A* 121:1940–1949
- [35] Li X, Claes P, Haertelt M, Lievens P, Janssens E, Fielicke A (2016) Structural determination of niobium-doped silicon clusters by far infrared spectroscopy and theory. *Phys Chem Chem Phys* 18:6291–6300
- [36] Kumar V (2008) *Nanosilico*. Elsevier, Amsterdam, pp 233–234
- [37] Lee C, Yang W, Parr RG (1998) Development of the Colle–Salvetti correlation energy formula into a functional of the electron density. *Phys Rev B* 37:785–789
- [38] Kresse G, Furthmüller J (1996) Efficient iterative schemes for ab initio total-energy calculations using a plane-wave basis set. *J Phys Rev B Condens Matter Mater Phys* 54:11169–11186
- [39] Kresse G, Joubert D (1999) From ultrasoft pseudopotentials to the projector augmented-wave method. *Phys Rev B Condens Matter Phys* 59:1758–1775
- [40] Frisch MJ, Trucks GW, Schlegel HB, Scuseria GE, Robb MA, Cheeseman JR, Zakrzewski VG, Montgomery JA Jr, Stratmann RE, Burant JC, Dapprich S, Millam JM, Daniels AD, Kudin KN, Strain MC, Farkas O, Tomasi J, Barone V, Cossi M, Cammi R, Mennucci B, Pomelli C, Adamo C, Clifford S, Ochterski J, Petersson GA, Ayala PY, Cui Q, Morokuma K, Malick DK, Rabuck AD, Raghavachari K, Foresman JB, Cioslowski J, Ortiz JV, Baboul AG, Stefanov BB, Liu B, Liashenko A, Piskorz P, Komaromi I, Al-Laham MA, Peng CY, Nanayakkara A, Challacombe M, Gill PMW, Johnson B, Chen W, Wong MW, Andres JL, Gonzalez C, Head-Gordon M, Replogle ES, Pople JA (2009) *Gaussian 09*. Gaussian Inc., Wallingford
- [41] Oganov AR, Glass CW (2006) Crystal structure prediction using ab initio evolutionary techniques: principles and applications. *J Chem Phys* 124:244704. <https://doi.org/10.1063/1.2210932>
- [42] Chen Z, Corminboeuf C, Heine T, Bohmann J, Schleyer PVR (2003) Do all metal antiaromatic clusters exist? *J Am Chem Soc* 125:13930–13931
- [43] Lombardi JR, Davis B (2002) Periodic properties of force constants of small transition metal and lanthanide clusters. *Chem Rev* 102:2431–2460
- [44] Northrup E, Cohen ML (1983) Predictions of the bond length and vibrational frequency of Ge_2 . *Chem Phys Lett* 102:440–441
- [45] Fillippou AC, Hoffmann D, Schnakenburg G (2017) Triple bonds of niobium with silicon, germanium and tin: the tetrylidyne complex $[(\text{K}3\text{-tmps})(\text{CO})_2\text{Nb} = \text{E-R}]$ ($\text{E} = \text{Si, Ge, Sn}$; $\text{tmps} = \text{MeSi}(\text{CH}_2\text{PMe}_2)_3$; $\text{R} = \text{aryl}$). *Chem Sci* 8:6290–6299
- [46] Goodwin L, Salahub DR (1993) Density-functional study of niobium clusters. *Phys Rev A* 47:774–777
- [47] Dmitry Yu, Zubarev Boris B, Averkiev Zhai HJ, Wang LS, Alexander IB (2008) Aromaticity and antiaromaticity in transition-metal systems. *Phys Chem Chem Phys* 10:257–267
- [48] Tai TB, Nguyen MT (2011) A stochastic search for the structures of small germanium clusters and their anions: enhanced stability by spherical aromaticity of the Ge_{10} and Ge_{122} -system. *J Chem Theor Comput* 7:1119–1130
- [49] Knight WD, Clemenger K, de Heer WA, Saunders WA, Chou MY, Cohen ML (1984) Electronic shell structure and abundances of sodium clusters. *Phys Rev Lett* 52:2141–2143
- [50] Clemenger K (1985) Ellipsoidal shell structure in free-electron metal clusters. *Phys Rev B* 32:1359–1362
- [51] De Heer WA (1993) The physics of simple metal clusters: experimental aspects and simple model. *Rev Mod Phys* 65:671–676
- [52] Khanna SN, Jena P (1995) Atomic clusters: building blocks for a class of solids. *Phys Rev B* 51:13705–13716
- [53] Kumar V (2013) High symmetry Nb_n and Ta_n ($n = 12, 15$, and 17) clusters: high magnetic moments and the finding of superatoms with doping. *Comput Theor Chem* 1021:149–154
- [54] Zhang M, Zhang J, Feng X, Zhang H, Zhao L, Luo Y, Cao W (2013) Magnetic superatoms in VLi_n ($n = 1\text{--}13$) clusters: a first principles prediction. *J Phys Chem C* 117:13025–13036